



Analysis of Influential Factors for the Relationship between PM_{2.5} and AOD in Beijing

Caiwang Zheng^{1,2}, Chuanfeng Zhao^{1,2*}, Yannian Zhu^{1,2,3*}, Yang Wang^{1,2}, Xiaoqin
Shi^{1,2}, Xiaolin Wu^{1,2}, Tianmeng Chen^{1,2}, Fang Wu^{1,2}, Yanmei Qiu^{1,2}

5

1. College of Global Change and Earth System Science, and State Key Laboratory of
Earth Surface Processes and Resource Ecology, Beijing 100875, China
2. Joint Center for Global Change Studies, Beijing, 100875, China
3. Meteorological Institute of Shaanxi Province, Xi' an, China

10

Correspondence to: Chuanfeng Zhao, czhao@bnu.edu.cn
Yannian Zhu, yannianzhu@gmail.com



Abstract: Relationship between aerosol optical depth (AOD) and $PM_{2.5}$ is often investigated in order to obtain surface $PM_{2.5}$ from satellite observation of AOD with a broad area coverage. However, various factors could affect the AOD- $PM_{2.5}$ regressions. Using both ground and satellite observations in Beijing from 2011 to 5 2015, this study analyzes the influential factors including the aerosol type, relative humidity (RH), atmospheric boundary layer height (PBLH), wind speed and direction, and the vertical structure of aerosol distribution. The ratio of $PM_{2.5}$ to AOD, which is defined as η , and the square of their correlation coefficient (R^2) have been examined. It shows that η varies from 54.32 to 183.14, 87.32 to 104.79, 95.13 to 163.52 and 1.23 10 to 235.08 $\mu\text{g}/\text{m}^3$ with aerosol type in four seasons respectively. η is smaller for scattering-dominant aerosols than for absorbing-dominant aerosols, and smaller for coarse mode aerosols than for fine mode aerosols. Both RH and PBLH affect the η value significantly. The higher the RH, the larger the η , and the higher the PBLH, the smaller the η . For AOD and $PM_{2.5}$ data with the correction of RH and PBLH 15 compared to those without, R^2 of monthly averaged $PM_{2.5}$ and AOD at 14:00 LT increases from 0.63 to 0.76, and R^2 of multi-year averaged $PM_{2.5}$ and AOD by time of day increases from 0.01 to 0.93, 0.24 to 0.84, 0.85 to 0.91 and 0.84 to 0.93 in four seasons respectively. Similar to the variation of AOD and $PM_{2.5}$, η also decreases with the increasing surface wind speed, indicating that the contribution of surface $PM_{2.5}$ 20 concentrations to AOD decreases with surface wind speed. The vertical structure of aerosol exhibits a remarkable change with seasons, with most particles concentrated



within about 500 m in summer and within 150 m in winter. Compared to the AOD of the whole atmosphere, AOD below 500 m has a better correlation with $PM_{2.5}$, for which R^2 is 0.77. This study suggests that all the above influential factors should be considered when we investigate the AOD- $PM_{2.5}$ relationships.

- 5 *Keywords:* $PM_{2.5}$ /AOD ratio, aerosol type, relative humidity (RH), atmospheric boundary layer height (PBLH), wind speed, aerosol vertical distribution.



1. Introduction

Atmospheric aerosols, also known as particulate matter, can influence the Earth's climate system by directly and indirectly modifying the incoming solar radiation and outgoing longwave radiation. The direct effect of aerosols on radiation refers to the absorption and scattering of the solar and longwave radiation by aerosols (Charlson et al., 1992; Koren et al., 2004; Lohmann and Feichter, 2005; Qian et al., 2007; Li et al., 2011; Huang et al., 2014; Yang et al., 2016) and the indirect effect of aerosols on radiation are associated with changes in the cloud macro- and micro-physical properties caused by aerosols which can serve as cloud condensation nuclei or ice nuclei (Twomey, 1977; Albrecht, 1989; Kaufman and Fraser, 1997; Feingold, 2003; Garrett et al., 2004; Garrett and Zhao, 2006; Zhao et al., 2012; Zhao and Garrett, 2015). The radiative effect of aerosols is relatively large due to increased emissions of pollution in East Asia (Wang et al., 2010a; Zhuang et al., 2013). Aerosols can also affect the precipitation intensity and patterns by changing cloud microphysical properties (Menon et al., 2002; Qian et al., 2009; Li et al., 2011; Guo et al., 2016a). Meanwhile, aerosols from anthropogenic pollution can cause serious impacts on atmospheric environment and human health by carrying hazardous materials (Pope et al., 2002; Zhang et al., 2007; Samoli et al., 2008; Xu et al., 2013). Thus, it is very important to get accurate information of aerosol properties, such as aerosol optical depth (AOD) and particle matter with size equal or smaller than 2.5 μm aerodynamic diameter ($\text{PM}_{2.5}$).



Aerosol properties are often obtained through satellite remote sensing, surface remote sensing, surface and aircraft in-situ observations. Remote sensing observation generally provides the aerosol optical properties such as aerosol extinction coefficient and AOD, but not the aerosol mass or number concentration. Differently, in-situ observations can provide direct measurements of aerosol concentration and PM_{2.5}. However, the limited samples for aircraft observation and limited sites for ground-based in-situ observation make it challenging to obtain the PM_{2.5} over many locations, particularly the spatial distribution. Recent studies have proposed methods to estimate the surface PM_{2.5} based on the AOD observations from satellites (van Donkellar et al., 2006, 2010, 2013; Drury et al., 2008; Wang et al., 2010b; Xin et al., 2016). Although PM_{2.5} from AOD has not high temporal resolution and is not available when it is cloudy or very pollutant, these methods provide the spatial distribution of PM_{2.5} globally or regionally.

Many studies have focused on the building of statistical regression models to derive the surface PM_{2.5} from AOD. For example, van Donkelaar et al. (2010) derived the global PM_{2.5} concentration distribution from satellite-derived AOD using the PM_{2.5}/AOD ratios obtained from a global chemical transport model (CTM). Xin et al. (2015) investigated the relationships between PM_{2.5} and AOD over China using the observations from the Campaign on atmospheric Aerosol Research-China network during the period from 2012 to 2013.

The relationships between PM_{2.5} and AOD show significant differences over



various locations (Corbin et al., 2002; Wang and Christopher, 2003; Hand et al., 2004; Ramachandran, 2005; Kumar et al., 2007; Zhang et al., 2009a; Ma et al., 2014). Some studies (e.g., Ma et al., 2014) have suggested that aerosol types and meteorological conditions can affect the relationship between $PM_{2.5}$ and AOD. However, systematic studies about the influential factors to the relationship between $PM_{2.5}$ and AOD have not been carried out, which are necessary for future derivation of accurate $PM_{2.5}$ from satellite AOD observations. Using both satellite and surface observation of aerosol properties and meteorology variables in Beijing from 2011 to 2015, this study analyzes the influential factors to AOD- $PM_{2.5}$ relationship, which includes aerosol type, relative humidity (RH), atmospheric planetary boundary layer height (PBLH), wind speed, and the vertical structure of aerosol distribution.

The paper is organized as follows. Section 2 describes the data and method. Section 3 analyzes the potential influential factors to AOD- $PM_{2.5}$ relationship, and section 4 summarizes the findings.

2. Data and Method

2.1 Data

The data used in this study are described as follows, including the data sources, their spatial and time resolutions, and so on. These data includes surface $PM_{2.5}$ concentrations and AOD, satellite-based AOD from the moderate-resolution imaging spectroradiometer (MODIS), satellite-based aerosol profiles from the Cloud-Aerosol



Lidar and Infrared Pathfinder Satellite Observation (CALIPSO), and meteorology data from China Meteorological Administration (CMA).

a. Ground $PM_{2.5}$ Measurements

The ground-based aerosol observation of $PM_{2.5}$ concentrations with hourly time resolution for the period of 2011 to 2015 is obtained from the U.S. Department of State at a single site (39.95 N, 116.47 E) in Beijing, as reported on the <http://www.stateair.net/> website. This data has relatively long time record, and has been widely used by many studies (Zheng et al., 2015; Jiang et al., 2015).

b. Meteorological Data

Meteorological parameters with 3-hour temporal resolution are provided by CMA, including cloud fraction (CF), 6-hour total precipitation (TP), relative humidity (RH), surface wind speed and wind direction. To eliminate the contamination of cloud and precipitation, data samples under cloudy ($CF \geq 0.1$) or rainy conditions ($TP > 0$) are removed. Same as Yang et al. (2016), we should note that even with this limitation, some days with few broken clouds ($CF < 0.1$) still can introduce additional uncertainties to our study. Planetary boundary layer heights (PBLH) are extracted from the European Centre for Medium-Range Weather Forecasts (ECMWF) interim reanalysis (ERA-Interim; Dee et al. 2011), with a horizontal resolution of $0.25^\circ \times 0.25^\circ$ and 3-hour temporal resolution. Guo et al. (2016b) have investigated the PBL in China from January 2011 to July 2015 using both the fine-resolution sounding observations and ECMWF reanalysis data. It was found that the seasonally averaged



BLHs derived from reanalysis are generally in good agreement with those of observations in Beijing. Considering this and that there are only 2 times sounding observations every day, the seasonally averaged ERA-BLHs have been used in this study.

5 *c. AERONET measurements*

The Aerosol Robotic Network (AERONET) program is a federation of ground-based remote sensing aerosol networks with more than 400 stations globally. At AERONET sites, the CE318 multiband sun-photometer is employed to measure spectral sun irradiance and sky radiances, from which AOD at 550 nm can be derived.

10 The AOD data has been processed into three quality levels: Level 1.0 (unscreened), Level 1.5 (cloud-screened), and Level 2.0 (cloud screened and quality-assured) (Holben et al., 1998). A detailed description about AERONET retrievals is discussed in Holben et al. (1998). In this study, Level 2.0 AOD at 550 nm, SSA at 675 nm and

15 AOD retrieved from AERONET are accurate to within ± 0.01 (Dubovik et al., 2000).

d. CALIOPSO profile products

CALIPSO is one part of A-Train, which is a constellation of satellites, tracking in a polar orbit and crossing the equator northbound at about 13:30 local time (LT) (Stephens et al. 2002). To investigate the characteristics of the aerosol vertical

20 distribution, aerosol extinction profiles at 532 nm from Version 3.01 CALIOP Level 2 5 km Aerosol Profile for the period of 2011 to 2015 are used, which are provided by



the CALIOP space borne lidar onboard the CALIPSO satellite (Winker et al., 2007, 2009; Hunt et al., 2009). The horizontal resolution is 5 km, and the vertical resolution varies with altitude. The CALIPSO columnar AOD is the integration of aerosol extinction coefficient with the altitude.

5 The extraction algorithm of the aerosol profile is shown in Fig. 1. First, the overpass time of CALIPSO satellite can be determined according to the geographical location of Beijing site (39.95°N, 116.47°E). Second, at each CALIPSO satellite pixel, AOD at each layer is derived as the multiplication of the extinction coefficient and layer depth. Finally, the AOD profiles inside 100 km radius region surrounding the
10 Beijing site is averaged as the final result. Note that when there are clouds or precipitation, the data are excluded in our analysis. Also, in this process, low-quality profiles in which *Extinction_Coefficient_Uncertainty_532* (*Sigma_Uncertainty* in Fig. 1) is greater than 99% and *COD* is greater than 0.1 have been excluded.

e. MODIS aerosol product

15 The MODIS instrument has a global coverage every one to two days with a viewing swath of 2330 km. It is operating on both the Terra and Aqua satellite, of which the overpass time are approximately 10:30 and 13:30 LT, respectively. To compare the AOD from MODIS and CALIPSO (only passes in the afternoon) observation, AOD from Terra (10:30 LT) are not used. Level 2 MODIS aerosol
20 product data (Collection 5.1) for the period of 2011 to 2015 are obtained from the Level-1 and Atmosphere Archive and Distribution System (LAADS DAAC), of which



the spatial resolution at nadir is 10 km×10 km (Levy et al., 2010). The AOD data (MODIS parameter name: Deep_Blue_Aerosol_Optical_Depth_Land) at 550 nm are used in this study.

2.2 Method

5 a. $PM_{2.5}/AOD$ ratio

AOD represents the total attenuation that aerosols of the whole atmosphere exert on solar radiation, while $PM_{2.5}$ mass concentrations measured by the ground monitoring site can only reflect the near-surface air quality condition. Based on the assumption of linear relationship between AOD (unitless) and $PM_{2.5}$ ($\mu\text{g}/\text{m}^3$), van Donkellar et al. (2010) has introduced a conversion factor (η), which can be defined as:

$$\eta = \frac{PM_{2.5}}{AOD} \quad (1)$$

where η ($\mu\text{g}/\text{m}^3$) indicates the optical thickness of aerosol particles per unit mass concentration. Its value depends on the aerosol type, aerosol size, RH, PBLH, and the vertical structure of aerosol distribution. At the same $PM_{2.5}$ concentration, if AOD is smaller, the extinction capability is weaker; if AOD is larger, the extinction capability is stronger. In other words, the larger the η , the weaker the aerosol extinction capability; the smaller the η , the stronger the aerosol extinction capability. Using this factor, we can study the dependence of $PM_{2.5}$ -AOD relationship (represented by η) on



different influential factors.

b. Aerosol Classification Method

Due to the difference of the sources, aerosols exhibit noticeable discrepancies in physical and optical properties with respect to the location and season. Fine-mode fraction (FMF) refers to the AOD fraction of fine-mode to the total. Angstrom exponent (AE) is an index reflecting the particulate size distribution of aerosols. Using FMF and AE, we can determine the dominant size mode of aerosols. We can also distinguish absorbing from non-absorbing aerosols based on measurements of single scattering albedo (SSA), which is defined as the ratio of the scattered
10 coefficient to the total attenuation coefficient.

In this study, hourly averaged level 2 inversion products from AERONET at sites in Beijing are used, including FMF, AE and SSA data. According to the radiation absorptivity and the size of aerosol particles (Lee, et al., 2010), aerosols are classified into six types as follows:

- 15 1) Coarse non-absorbing ($SSA > 0.95$, $FMF \leq 0.4$ and $AE \leq 0.6$)
- 2) Coarse absorbing ($SSA \leq 0.95$, $FMF \leq 0.4$ and $AE \leq 0.6$)
- 3) Fine non-absorbing ($SSA > 0.95$, $FMF > 0.6$ and $AE > 1.2$)
- 4) Fine absorbing ($SSA \leq 0.95$, $FMF > 0.6$ and $AE > 1.2$)
- 5) Mixed non-absorbing ($SSA > 0.95$, $0.4 \leq FMF < 0.6$ and $0.6 \leq AE < 1.2$)
- 20 6) Mixed absorbing ($SSA \leq 0.95$, $0.4 \leq FMF < 0.6$ and $0.6 \leq AE < 1.2$)



Coarse absorbing and fine absorbing aerosols are considered as dust and black carbon (BC) respectively. Since the high percentage of fine mode absorbing aerosol, it is further divided into heavily ($SSA \leq 0.85$), moderately ($0.85 < SSA \leq 0.9$) and slightly ($0.9 < SSA \leq 0.95$) absorbing aerosols. Fig. 2 shows the aerosol type classification performed using SSA, FMF and AE from AERONET at sites in Beijing using the method described above. Roughly, the aerosols are mainly fine mode slightly absorbing and non-absorbing particles in summer, and fine mode slightly and moderately absorbing particles in winter. The coarse mode dust aerosols mainly occurs in spring (MAM) and winter (DJF).

10 **3. Analysis and Results**

3.1 AOD

We first evaluate the uncertainties in the satellite observed AOD using the ground observations from AERONET at the satellite passing time, including both MODIS and CALIPSO at 13:30 LT. Based on the satellite overpass time, the corresponding AERONET AOD in time within 30-min are compared to MODIS AOD and CALIPSO AOD respectively, which is shown in Fig. 3. The correlation between MODIS and AERONET AOD is significant ($R^2 = 0.85$, $N = 415$), with a slope of 1.32 and an RMS error of 0.23, indicating that MODIS AOD is biased high compared to AERONET AOD. In contrast, the correlation between CALIPSO and AERONET AOD is slightly lower than that between MODIS and AERONET ($R^2 = 0.65$, $N = 70$),



with a slope of 0.78 and a RMS error of 0.31. In general, the CALIPSO AOD is biased low compared to AERONET AOD.

Table 1 further shows the inter-comparison results of AOD between AERONET and MODIS in spring (MAM), summer (JJA), fall (SON) and winter (DJF). MODIS has a substantial positive bias in spring, summer and fall (36.7, 44.7 and 32.9%), but a smaller positive bias in winter (10.2%). MODIS correlates best with AERONET in spring and summer, of which R^2 is 0.81 and 0.87. When the AOD becomes small, it seems that the correlation of AOD between MODIS and AERONET also decreases.

Same as Table 1, Table 2 shows the inter-comparison results of AOD between AERONET and CALIPSO in spring, summer, fall and winter. The correlation (R^2) between CALIPSO and AERONET AOD are 0.52, 0.48, 0.85 and 0.55 respectively in four seasons. CALIPSO AOD has a positive bias in summer and winter (6.6 and 25.0%), but a negative bias in spring and fall (-5.2 and -14.2%). For all seasons, RMSE are less for MODIS than CALIPSO compared to AERONET. The results shown in Fig. 2 and Tables 1 and 2 indicate that considerable uncertainties exist in the satellite observed AOD, introducing up to 45% errors (seasonal biases 5-45%) to the quantification of AOD-PM_{2.5} relationships.

3.2 Effect of RH and PBLH

Relative humidity, by affecting the water uptake process of aerosols, can cause a pronounced change to the aerosol size distribution, chemical composition, and the



extinction characteristics (Liu et al., 2008). The hygroscopic growth factor, defined as $f(RH)$, denotes the ratio of the aerosol scattering coefficients in ambient with a certain RH to that in dry air conditions (Li et al., 2014). In this article, $f(RH)$ is expressed as follows in a simple function:

$$5 \quad f(RH) = \frac{1}{(1 - RH / 100)} \quad (2)$$

The hygroscopic growth process causes the overestimation of the AOD, since the columnar AOD is derived under ambient conditions. An adjusting dehydration process is needed, which can be described as:

$$AOD_{dry} = \frac{AOD}{f(RH)} \quad (3)$$

10 where AOD_{dry} represents the aerosol optical depth with dehydration adjustment.

PBLH influences the vertical profile of particulate matters. In general, the PBLH is dependent on many factors, including meteorological conditions, terrain, sensible heat flux, evaporation and ground roughness (Stull, 1988). Based on the assumption that the air is uniformly mixed and aerosol particles are evenly distributed in the
15 boundary layer, the column integrated $PM_{2.5}$ concentration ($PM_{2.5_column}$) within PBLH can be approximated as:

$$PM_{2.5_column} = PM_{2.5} \times PBLH \quad (4)$$

Previous studies have shown that aerosols are mainly concentrated within the PBL (Guinot et al., 2006; Zhang et al., 2009b). Here, we assume that the column
20 integrated $PM_{2.5}$ within PBLH should be comparable to the whole column integrated



PM_{2.5}. Eqs. (3) and (4) imply that the increase of RH can result in the increase of AOD and the decrease of η , and that the increase of PBLH can cause the decrease of near-surface PM_{2.5} concentrations and the decrease of η . Actually, PBLH often correlates with RH, making the separation of PBLH and RH effects challenging. Here, we simply show the effects of both PBLH and RH on the AOD-PM_{2.5} relationship.

Fig. 4(a) shows the time series of PBLH (km) and RH (%). It's clear to see an opposite trend between PBLH and RH. The averaged PBLH for 2011 to 2015 are 2.56 km, 1.97 km, 1.55 km and 1.32 km respectively in MAM, JJA, SON and DJF, of which the corresponding averaged RH are 27.58%, 48.73%, 42.78% and 33.05%. In May, PBLH has the highest value above 2.5 km, and in July, RH has the highest value above 50%. The opposite trend between PBLH and RH shown in Fig. 6(a) implies that AOD-PM_{2.5} relationship could be improved a lot while both of their effects are considered.

Fig. 4(b) shows the temporal variation of monthly averaged AOD and PM_{2.5} at 14:00 LT without any meteorology-based modification to the original observations. It shows a good positive relationship in the time variations of monthly averaged AOD and PM_{2.5} with a high correlation ($R^2 = 0.63$). Although the temporal trend of AOD and PM_{2.5} are basically consistent, AOD are considerably higher in MAM and JJA while PM_{2.5} lower in JJA. That's because in MAM, PBLH is high and the vertical mixing of aerosols makes near-surface PM_{2.5} concentrations low, while in JJA, RH is high and the hygroscopic growth of aerosols lead to the increase of AOD.



Fig. 4(c) further shows the temporal variation of monthly averaged AOD_{dry} and $PM_{2.5_column}$ at 14:00 LT which have been adjusted based on Eqs. (3) and (4). It shows much better positive relationship in the temporal variation of monthly averaged AOD_{dry} and $PM_{2.5_column}$, with R^2 as 0.74. This promising result indicates that the

5 PBLH and RH corrections are essential for the improvement of the retrieval accuracy of $PM_{2.5}$ from AOD.

Fig. 5 compares the diurnal variation of RH and PBLH over four seasons averaged from 2011 to 2015 in Beijing. In terms of seasonal difference, PBLH is the highest in MAM, followed by JJA and SON, the lowest in DJF, which is consistent

10 with the results found by Guo et al. (2016b). In spring, high PBLH may be associated with the climatologically strongest near-surface wind speed, while in summer, high PBLH is contributed to the strong solar radiation (Guo et al., 2016b). RH is the highest in summer, followed by fall and winter, the lowest in spring. In terms of diurnal variation, it can be seen that from 8:00 to 14:00 LT, the solar radiation that

15 surface receives increases, making PBLH rises and RH decreases gradually; PBLH at 14:00 LT is the highest and RH at 14:00 LT is the lowest within the whole day. However, from 14:00 to 20:00 LT, the solar radiation that surface receives reduces, thus PBLH goes down and RH increases gradually. PBLH is the lowest and RH is the highest at 23:00 and 2:00 LT respectively within the whole day.

20 Fig. 6 shows the diurnal variation of multi-year (2011-2015) averaged RH and PBLH, AOD and $PM_{2.5}$, AOD_{dry} and $PM_{2.5_column}$ in four seasons. The columns



represent four seasons of spring, summer, fall and winter and the rows represent different variables. Fig. 6(a1-d1) show that PBLH and RH demonstrate a steady increase and decrease trend from 6:00 to 17:00 LT, respectively. As shown in Fig. 6(a2)-(d2), the AOD-PM_{2.5} linear relationship shows that R² are 0.01, 0.24, 0.85 and 5 0.84 in four seasons respectively. After PBLH and RH corrections (Fig. 6(a3-d3)), it shows that R² between AOD_{dry} and PM_{2.5,column} are 0.93, 0.84, 0.91, 0.93 in four seasons respectively. These results further indicate that RH and PBLH play essential roles for AOD-PM_{2.5} relationship.

3.2 Aerosol type

10 To study the influence of aerosol type on η , we analyze the data from 11:00 to 17:00 LT in four seasons respectively. By doing this, we try to limit the influence of diurnal and seasonal variation of RH and PBLH on η . The aerosol types can be classified based on the aerosol particle size and radiative absorptivity, and η is a good indicator to the extinction capability of different aerosol types.

15 Fig. 7 depicts the seasonal frequency distribution of aerosol types in four seasons at Beijing for the period of 2011 to 2015. Dust accounts for 15.4%, 0.4%, 6.4% and 6.9% in spring (MAM), summer (JJA), fall (SON) and winter (DJF) respectively. Same as that indicated from Fig. 1, dust aerosols is heavy in spring and winter, particularly in spring. Higher proportion of dust in spring is mainly associated with
20 the long-range transport from northwest arid areas (Yan et al., 2015, Tan et al., 2012).



Fine mode absorbing aerosols account for 36.5%, 42.6%, 51.1% and 60.3% in four seasons respectively, of which moderately absorbing aerosols account for the highest. Owing to the biomass burning and soot emission generated from heating, the fine mode heavily-absorbing aerosol percentage is higher in winter than in other seasons, which is 7.7%. The content of heavily non-absorbing aerosols is significantly higher in summer and fall than in other two seasons, particularly in summer with a value of 48.4%. As a whole, the aerosol particles in Beijing are primarily fine-mode and absorbing aerosols in terms of particle size and optical property.

Fig. 8 presents the variation of η with the aerosol type by season in Beijing. Note that there are too few coarse-mode cases in summer and the corresponding η is a missing value. η generally decrease with particle size, with the smallest value for coarse-mode aerosols and largest value for fine-mode aerosols, and it seems that η of non-absorbing aerosols is smaller than absorbing aerosols. This implies that the aerosol extinction capacity increases with particle size, and it is stronger for the non-absorbing aerosols than absorbing aerosols.

Table 3 further compares the AERONET hourly averaged AOD to $PM_{2.5}$ mass concentrations by aerosol type. Coarse Non-absorbing aerosols show the lowest correlation between AOD and $PM_{2.5}$, of which R^2 is 0.10. For all kinds of aerosols, the correlation between AOD and $PM_{2.5}$ is relatively lower than that for aerosols with a specific type other than coarse non-absorbing, of which R^2 is 0.51 and RMS error is $46.34 \mu\text{g}/\text{m}^3$.



Fig. 9 shows the difference in the relationship of $PM_{2.5}$ and AOD among six different aerosol types by season. For all types of aerosols, the slopes of the linear regression functions ($PM_{2.5}=a \times AOD+b$) are 90.16, 56.9, 117.97 and 138.42 in four seasons respectively. The seasonal differences of the slope are attributed to the effect of PBLH and RH. In summer, high RH brings about the hygroscopic growth of aerosol, thus increasing the extinction efficiency of aerosols and then reducing the slope. Differently, in winter, low PBLH value increases the contribution of surface $PM_{2.5}$ to the columnar AOD, thus increasing the slope. The slopes in spring and autumn fall in between. However, there are large differences in the slope of regression functions among different aerosol types, which varies from 13.75 to 111.09, 40.04 to 204.45, 70.79 to 130.56 and 43.58 to 157.93 $\mu g/m^3$ in four seasons respectively. Same as shown in Fig. 4, the slope decreases with particle size, with smallest value for coarse-mode aerosols and largest value for fine-mode aerosols in four seasons, and the slope of non-absorbing aerosols is generally smaller than absorbing aerosols.

The findings in this section implies that AOD- $PM_{2.5}$ relationship varies considerably with aerosol types. When we investigate the relationship between $PM_{2.5}$ and AOD, the aerosol types should be carefully considered for study regions.

3.4 Wind

This section discusses how wind affects the AOD- $PM_{2.5}$ relationship in two aspects: wind direction and surface wind speed. Surrounded by Hebei province with



severe pollution, Beijing is affected by the long-range transport of aerosols. The seasonal variation of wind direction changes the transport and spatial-temporal distribution of aerosols originated from different sources with distinctive physicochemical characteristics, which has a direct influence on the AOD-PM_{2.5} relationship.

Fig. 10 describes the wind rose of Beijing in four seasons for the period from 2011 to 2015. Surface wind speed is mainly distributed in the range of 0 to 9 m/s. Wind direction is mainly southwest in spring and summer, northeast in fall and northwest in winter. There are more windy days in spring and winter. The northwest wind in spring causes the transport of dust aerosols from gobi and desert regions of China to Beijing. The occurrence frequency of stable weather ($v=0$ m/s) are 4.2%, 5.8%, 9.2% and 8.3% in spring, summer, fall and winter, respectively. Different from the wind speed which will be analyzed in Figs. 11 and 12, the influence of wind direction to the AOD-PM_{2.5} relationship is not significant, at least in this study, which is worthy for further study in the future.

Fig. 11 illustrates the relationship between the severity extent of haze with surface wind speed. For good air quality ($PM_{2.5}<50$ $\mu\text{g}/\text{m}^3$), the occurrence rate increases with increasing wind speed, ranging from 39.3% ($v\leq 1$ m/s) to 92.9% ($v>7$ m/s). Differently, the occurrence of poor air quality ($PM_{2.5}>150$ $\mu\text{g}/\text{m}^3$) ranges from 20.92% ($v\leq 1$ m/s) to 0 ($v>7$ m/s). The weakening of surface wind speed reduces the



transport of near-surface haze to the outside regions, leading to the build-up and
continuance of heavy haze weather in Beijing. On the contrary, the increase of surface
wind speed, which may be due to the development of weather system like monsoon in
Beijing, causes the disperse of aerosols, and then reduction of the heavy haze
5 occurrence rate.

Fig. 12 describes the variation of averaged AOD, $PM_{2.5}$ and η with surface wind
speed. Although AOD and $PM_{2.5}$ are basically consistent in the decrease trend with the
increasing surface wind speed, AOD variation is more complicated and less sensitive
to surface wind speed. Compared with the $PM_{2.5}$ variation range of 10~110 $\mu\text{g}/\text{m}^3$, the
10 variation range of AOD is between 0.2 and 0.6. This is likely associated with the fact
that the columnar AOD is affected by many factors, and the surface wind speed is just
a disturbing term to surface $PM_{2.5}$. Similar to the variation of AOD and $PM_{2.5}$, η also
decreases with the increasing surface wind speed, indicating that the contribution of
surface $PM_{2.5}$ concentrations to AOD decreases with surface wind speed.

15 3.5 Vertical distribution of aerosols

It has indicated that the relationship between AOD and $PM_{2.5}$ varies with the
surface wind speed and the surface aerosol amount. Considering that AOD is the
vertical integration of aerosol optical properties, the AOD- $PM_{2.5}$ relationship should
vary with the vertical distribution of aerosols. We examine this by using the extinction
20 profiles in 532 nm band from the Version 3.01 CALIOP Level 2 5 km Aerosol Profile



product from 2011 to 2015.

Fig. 13 shows the CALIPSO aerosol optical depth vertical distribution profile and cumulative distribution with height in four seasons. Fig. 13(a) shows that there are different AOD vertical distribution patterns among four seasons. The maximum
5 AOD occurs at different heights as described later in Fig. 14. These different vertical patterns could make the AOD-PM_{2.5} relationship vary with season. Fig. 13(b) further shows that cumulative AOD is very different in summer from other seasons, with more concentrated at high heights.

Fig.14 shows the probability density distribution function (PDF) of AOD with
10 altitude in four different seasons. Within the atmospheric boundary layer, the main air movement form is the turbulent motion, promoting the vertical exchanges of heat, water vapor, momentum and various kinds of materials including aerosol pollutants. The turbulent energy is generally dependent on both the buoyancy and wind shear, particularly the buoyancy which is highly related to surface downwelling radiation.
15 Obviously, compared to other seasons, the solar radiation received by the surface is more in summer, and the turbulence is stronger, making aerosol transfer to a higher altitude. As expected and that shown in Fig. 13 (a), the vertical distribution of AOD is highly different in four seasons, implying different AOD-PM_{2.5} relationships. The height h with peak AOD is 516.8 m in summer, higher than that in other seasons,
20 indicating that the aerosols are mainly distributed in heights below ~500 m. The height h with peak AOD is about 337 and 277 m in spring and fall, respectively. In



winter, the surface receives the least amount of solar radiation, leading to weak turbulence. Correspondingly, h with peak AOD is only 158 m in winter, indicating that the aerosols are mainly distributed near the surface layer, contributing to heavy haze events in this season.

5 The significant time variation of the aerosol vertical distribution makes it one of key factors to influence the AOD-PM_{2.5} relationship. We next examine the relationship between AOD from surface to different heights and PM_{2.5} at surface. By defining AOD below a height as the integration of extinction coefficients vertically from surface to that height, the ratio of AOD below a specific height to the total AOD
10 can be determined by CALIPSO vertical profile, which is

$$AOD_H = AOD_{AeronetTotal} \times \frac{AOD_{CalipsoBelowH}}{AOD_{CalipsoTotal}} \quad (5)$$

where $AOD_{AeronetTotal}$ is AOD derived by AERONET, $AOD_{CalipsoTotal}$ is the total AOD from CALIPSO. $AOD_{CalipsoBelowH}$ is AOD below H from CALIPSO. AOD_H is the AOD below H .

15 We here examine four heights, which are 500 m, 1000 m, PBLH and top of atmosphere. Note that PBLH is not constant, but varies with time. Fig. 15 shows linear relationships between AOD below these four heights and PM_{2.5} at surface. For four heights of 500 m, 1000 m, PBLH and top of atmosphere, we can see that the correlation between AOD below and surface PM_{2.5} decreases with selected heights,
20 with R² of 0.77, 0.76, 0.66 and 0.64 respectively. More clearly, the slopes of linear regression lines vary a lot for heights 500 m, 1000 m and PBLH, but much smaller for



H above PBLH. This further implies that most of aerosols concentrate within PBLH in the atmosphere, and the variation of aerosol vertical distribution could introduce large uncertainties to AOD-PM_{2.5} relationship.

4. Summary

5 This study analyzes the various factors that affect the AOD-PM_{2.5} relationship qualitatively or quantitatively, including the satellite AOD observation, aerosol type, RH, PBLH, wind direction and speed, and the aerosol vertical distribution. It shows all of these factors can change the AOD-PM_{2.5} relationship, with different contributions. AOD from MODIS and CALIPSO are evaluated against the AERONET
10 data. The MODIS and AERONET AOD correlation is significant ($R^2 = 0.85$, $N = 415$), with a slope of 1.32 and a RMS error of 0.23, indicating that AOD is higher from MODIS than that from AERONET. In contrast, the correlation of AOD between CALIPSO and AERONET is slightly lower ($R^2 = 0.65$, $N = 70$), with a slope of 0.78 and a RMS error of 0.31.

15 There are large differences in the seasonal and diurnal variation of PBLH and RH. In Beijing, PBLH is the highest in spring, followed by summer and fall, the lowest in winter, and RH is the highest in summer, followed by fall and winter, the lowest in spring. For AOD and PM_{2.5} data with the correction of RH and PBLH compared to those without, R^2 of monthly averaged PM_{2.5} and AOD at 14:00 LT
20 increases from 0.63 to 0.76, and R^2 of multi-year averaged PM_{2.5} and AOD by time of day increases from 0.01 to 0.93, 0.24 to 0.84, 0.85 to 0.91 and 0.84 to 0.93 in four



seasons respectively.

The aerosol particles in Beijing are primarily fine-mode and absorbing aerosols in terms of particle size and optical property. Due to the long-range transport of aerosols from northwest arid areas, dust aerosols is heavy in spring and winter, particularly in spring. It shows that η varies from 54.32 to 183.14, 87.32 to 104.79, 95.13 to 163.52 and 1.23 to 235.08 $\mu\text{g}/\text{m}^3$ with the aerosol type in spring, summer, fall and winter, respectively. η is generally smaller for scattering-dominant aerosols than for absorbing-dominant aerosols, and smaller for coarse mode aerosols than for fine mode aerosols.

The surface wind speed significantly affects the occurrence of haze events. For good air quality ($\text{PM}_{2.5} < 50 \mu\text{g}/\text{m}^3$), the occurrence rate increases with increasing wind speed, ranging from 39.3% ($v \leq 1 \text{ m/s}$) to 92.9% ($v > 7 \text{ m/s}$). Differently, the occurrence of poor air quality ($\text{PM}_{2.5} > 150 \mu\text{g}/\text{m}^3$) ranges from 20.92% ($v \leq 1 \text{ m/s}$) to 0 ($v > 7 \text{ m/s}$). It shows that η decreases with the increasing surface wind speed, indicating that the contribution of surface $\text{PM}_{2.5}$ concentrations to AOD decreases with surface wind speed.

The vertical structure of aerosol distribution exhibits a remarkable change with seasons, which could also contribute a lot to the AOD- $\text{PM}_{2.5}$ relationship. This study shows that aerosols mainly concentrate within about 500 m height in summer, while concentrate within the surface layer of around 150 m height in winter in Beijing. Compared to the AOD of the whole atmosphere, AOD below 500 m has a better



correlation with $PM_{2.5}$, of which R^2 is 0.77 and RMSE is $38.6 \mu\text{g}/\text{m}^3$.

Acknowledgements

This work was supported by the National Natural Science Foundation of China (NSFC: grant 41575143), the Ministry of Science and Technology of China (grants 20
5 13CB955802), the China "1000 Plan" young scholar program, and the Chinese Program for New Century Excellent Talents in University (NCET). Sincerest thanks to the AERONET, MODIS and CALIPSO teams for their datasets. The CALIPSO data were obtained from the NASA Langley Research Center Atmospheric Science Data Center. Special thanks to the U.S. Embassy and CMA providing the $PM_{2.5}$ data and
10 meteorological data respectively.



References

- Alebrecht, B. A.: Aerosols, cloud microphysics, and fractional cloudiness, *SCIENCE*, 245, 1227-1230, 10.1126/science.245.4923.1227, 1989.
- Charlson, R. J., Schwartz, S. E., Hales, J. M., Cess, R. D., Coakley, J. A., Hansen, J. E., and Hofmann, D. J.: Climate forcing by anthropogenic aerosols, *SCIENCE*, 5 255, 423-430, 10.1126/science.255.5043.423, 1992.
- Corbin, K. C., Kreidenweis, S. M., and Vonder Haar, T. H.: Comparison of aerosol properties derived from Sun photometer data and ground-based chemical measurements, *GEOPHYSICAL RESEARCH LETTERS*, 29, 10 10.1029/2001gl014105, 2002.
- Dee, D. P., Uppala, S. M., Simmons, A. J., Berrisford, P., Poli, P., Kobayashi, S., Andrae, U., Balmaseda, M. A., Balsamo, G., Bauer, P., Bechtold, P., Beljaars, A. C. M., van de Berg, L., Bidlot, J., Bormann, N., Delsol, C., Dragani, R., Fuentes, M., Geer, A. J., Haimberger, L., Healy, S. B., Hersbach, H., Holm, E. V., Isaksen, 15 L., Kallberg, P., Koehler, M., Matricardi, M., McNally, A. P., Monge-Sanz, B. M., Morcrette, J. J., Park, B. K., Peubey, C., de Rosnay, P., Tavolato, C., Thepaut, J. N., and Vitart, F.: The ERA-Interim reanalysis: configuration and performance of the data assimilation system, *QUARTERLY JOURNAL OF THE ROYAL METEOROLOGICAL SOCIETY*, 137, 553-597, 10.1002/qj.828, 2011.
- 20 Drury, E., Jacob, D. J., Wang, J., Spurr, R. J. D., and Chance, K.: Improved algorithm for MODIS satellite retrievals of aerosol optical depths over western North



- America, JOURNAL OF GEOPHYSICAL RESEARCH-ATMOSPHERES, 113,
10.1029/2007jd009573, 2008.
- Dubovik, O., Smirnov, A., Holben, B. N., King, M. D., Kaufman, Y. J., Eck, T. F., and
Slutsker, I.: Accuracy assessments of aerosol optical properties retrieved from
5 Aerosol Robotic Network (AERONET) Sun and sky radiance measurements,
JOURNAL OF GEOPHYSICAL RESEARCH-ATMOSPHERES, 105,
9791-9806, 10.1029/2000jd900040, 2000.
- Feingold, G.: Modeling of the first indirect effect: Analysis of measurement
requirements, GEOPHYSICAL RESEARCH LETTERS, 30,
10 10.1029/2003gl017967, 2003.
- Garrett, T. J., Zhao, C., Dong, X., Mace, G. G., and Hobbs, P. V.: Effects of varying
aerosol regimes on low-level Arctic stratus, GEOPHYSICAL RESEARCH
LETTERS, 31, 10.1029/2004gl019928, 2004.
- Garrett, T. J., and Zhao, C. F.: Increased Arctic cloud longwave emissivity associated
15 with pollution from mid-latitudes, NATURE, 440, 787-789,
10.1038/nature04636, 2006.
- Green, M., Kondragunta, S., Ciren, P., and Xu, C.: Comparison of GOES and MODIS
Aerosol Optical Depth (AOD) to Aerosol Robotic Network (AERONET) AOD
and IMPROVE PM_{2.5} Mass at Bondville, Illinois, JOURNAL OF THE AIR &
20 WASTE MANAGEMENT ASSOCIATION, 59, 1082-1091,
10.3155/1047-3289.59.9.1082, 2009.



- Guinot, B., Roger, J.-C., Cachier, H., Wang, P., Bai, J., and Tong, Y.: Impact of vertical atmospheric structure on Beijing aerosol distribution, *ATMOSPHERIC ENVIRONMENT*, 40, 5167-5180, 10.1016/j.atmosenv.2006.03.051, 2006.
- Guo, J., Deng, M., Lee, S. S., Wang, F., Li, Z., Zhai, P., Liu, H., Lv, W., Yao, W., and
5 Li, X.: Delaying precipitation and lightning by air pollution over the Pearl River Delta. Part I: Observational analyses, *JOURNAL OF GEOPHYSICAL RESEARCH-ATMOSPHERES*, 121, 6472-6488, 10.1002/2015jd023257, 2016a.
- Guo, J., Miao, Y., Zhang, Y., Liu, H., Li, Z., Zhang, W., He, J., Lou, M., Yan, Y., Bian,
L., and Zhai, P.: The climatology of planetary boundary layer height in China
10 derived from radiosonde and reanalysis data, *ATMOSPHERIC CHEMISTRY AND PHYSICS*, 16, 13309-13319, 10.5194/acp-16-13309-2016, 2016b.
- Hand, J. L., Kreidenweis, S. M., Slusser, J., and Scott, G.: Comparisons of aerosol optical properties derived from Sun photometry to estimates inferred from surface measurements in Big Bend National Park, Texas, *ATMOSPHERIC
15 ENVIRONMENT*, 38, 6813-6821, 10.1016/j.atmosenv.2004.09.004, 2004.
- Holben, B. N., Eck, T. F., Slutsker, I., Tanre, D., Buis, J. P., Setzer, A., Vermote, E., Reagan, J. A., Kaufman, Y. J., Nakajima, T., Lavenu, F., Jankowiak, I., and Smirnov, A.: AERONET - A federated instrument network and data archive for aerosol characterization, *REMOTE SENSING OF ENVIRONMENT*, 66, 1-16,
20 10.1016/s0034-4257(98)00031-5, 1998.
- Huang, J., Wang, T., Wang, W., Li, Z., and Yan, H.: Climate effects of dust aerosols



- over East Asian arid and semiarid regions, *JOURNAL OF GEOPHYSICAL RESEARCH-ATMOSPHERES*, 119, 11398-11416, 10.1002/2014jd021796, 2014.
- Hunt, W. H., Winker, D. M., Vaughan, M. A., Powell, K. A., Lucker, P. L., and
5 Weimer, C.: CALIPSO Lidar Description and Performance Assessment, *JOURNAL OF ATMOSPHERIC AND OCEANIC TECHNOLOGY*, 26, 1214-1228, 10.1175/2009jtecha1223.1, 2009.
- Jiang, J., Zhou, W., Cheng, Z., Wang, S., He, K., and Hao, J.: Particulate Matter
Distributions in China during a Winter Period with Frequent Pollution Episodes
10 (January 2013), *AEROSOL AND AIR QUALITY RESEARCH*, 15, 494-U157, 10.4209/aaqr.2014.04.0070, 2015.
- Kaufman, Y. J., and Fraser, R. S.: The effect of smoke particles on clouds and climate
forcing, 5332, 1636-1639 pp., 1997.
- Koren, I., Kaufman, Y. J., Remer, L. A., and Martins, J. V.: Measurement of the effect
15 of Amazon smoke on inhibition of cloud formation, *SCIENCE*, 303, 1342-1345, 10.1126/science.1089424, 2004.
- Kumar, N., Chu, A., and Foster, A.: An empirical relationship between $PM_{2.5}$ and
aerosol optical depth in Delhi Metropolitan, *ATMOSPHERIC ENVIRONMENT*,
41, 4492-4503, 10.1016/j.atmosenv.2007.01.046, 2007.
- 20 Lee, J., Kim, J., Song, C. H., Kim, S. B., Chun, Y., Sohn, B. J., and Holben, B. N.:
Characteristics of aerosol types from AERONET sunphotometer measurements,



- ATMOSPHERIC ENVIRONMENT, 44, 3110-3117,
10.1016/j.atmosenv.2010.05.035, 2010.
- Levy, R. C., Remer, L. A., Kleidman, R. G., Mattoo, S., Ichoku, C., Kahn, R., and Eck,
T. F.: Global evaluation of the Collection 5 MODIS dark-target aerosol products
5 over land, ATMOSPHERIC CHEMISTRY AND PHYSICS, 10, 10399-10420,
10.5194/acp-10-10399-2010, 2010.
- Li, J., Han, Z., and Zhang, R.: Influence of aerosol hygroscopic growth
parameterization on aerosol optical depth and direct radiative forcing over East
Asia, ATMOSPHERIC RESEARCH, 140, 14-27,
10 10.1016/j.atmosres.2014.01.013, 2014.
- Li, Z., Niu, F., Fan, J., Liu, Y., Rosenfeld, D., and Ding, Y.: Long-term impacts of
aerosols on the vertical development of clouds and precipitation, NATURE
GEOSCIENCE, 4, 888-894, 10.1038/ngeo1313, 2011.
- Liu, X., Cheng, Y., Zhang, Y., Jung, J., Sugimoto, N., Chang, S.-Y., Kim, Y. J., Fan, S.,
15 and Zeng, L.: Influences of relative humidity and particle chemical composition
on aerosol scattering properties during the 2006 PRD campaign,
ATMOSPHERIC ENVIRONMENT, 42, 1525-1536,
10.1016/j.atmosenv.2007.10.077, 2008.
- Lohmann, U., and Feichter, J.: Global indirect aerosol effects: a review,
20 ATMOSPHERIC CHEMISTRY AND PHYSICS, 5, 715-737, 2005.
- Ma, Z., Hu, X., Huang, L., Bi, J., and Liu, Y.: Estimating ground-Level PM_{2.5} in China



- using satellite remote sensing, ENVIRONMENTAL SCIENCE &
TECHNOLOGY, 48, 7436-7444, 10.1021/es5009399, 2014.
- Menon, S., Hansen, J., Nazarenko, L., and Luo, Y. F.: Climate effects of black carbon
aerosols in China and India, SCIENCE, 297, 2250-2253,
5 10.1126/science.1075159, 2002.
- Pope, C. A., Burnett, R. T., Thun, M. J., Calle, E. E., Krewski, D., Ito, K., and
Thurston, G. D.: Lung cancer, cardiopulmonary mortality, and long-term
exposure to fine particulate air pollution, JAMA-JOURNAL OF THE
AMERICAN MEDICAL ASSOCIATION, 287, 1132-1141,
10 10.1001/jama.287.9.1132, 2002.
- Qian, Y., Wang, W., Leung, L. R., and Kaiser, D. P.: Variability of solar radiation
under cloud-free skies in China: The role of aerosols, GEOPHYSICAL
RESEARCH LETTERS, 34, 10.1029/2006gl028800, 2007.
- Qian, Y., Gong, D., Fan, J., Leung, L. R., Bennartz, R., Chen, D., and Wang, W.:
15 Heavy pollution suppresses light rain in China: Observations and modeling,
JOURNAL OF GEOPHYSICAL RESEARCH-ATMOSPHERES, 114,
10.1029/2008jd011575, 2009.
- Ramachandran, S.: PM_{2.5} mass concentrations in comparison with aerosol optical
depths over the Arabian Sea and Indian Ocean during winter monsoon,
20 ATMOSPHERIC ENVIRONMENT, 39, 1879-1890,
10.1016/j.atmosenv.2004.12.003, 2005.



- Samoli, E., Peng, R., Ramsay, T., Pipikou, M., Touloumi, G., Dominici, F., Burnett, R.,
Cohen, A., Krewski, D., Samet, J., and Katsouyanni, K.: Acute Effects of
Ambient Particulate Matter on Mortality in Europe and North America: Results
from the APHENA Study, ENVIRONMENTAL HEALTH PERSPECTIVES, 116,
5 1480-1486, 10.1289/ehp.11345, 2008.
- Stephens, G. L., Vane, D. G., Boain, R. J., Mace, G. G., Sassen, K., Wang, Z. E.,
Illingworth, A. J., O'Connor, E. J., Rossow, W. B., Durden, S. L., Miller, S. D.,
Austin, R. T., Benedetti, A., and Mitrescu, C.: The cloudsat mission and the
a-train - A new dimension of space-based observations of clouds and
10 precipitation, BULLETIN OF THE AMERICAN METEOROLOGICAL
SOCIETY, 83, 1771-1790, 10.1175/bams-83-12-1771, 2002.
- Stull, R. B.: An introduction to boundary layer meteorology, Kluwer Academic
Publishers, Dordrecht, 670 pp., 1988.
- Tan, S.-C., Shi, G.-Y., and Wang, H.: Long-range transport of spring dust storms in
15 Inner Mongolia and impact on the China seas, ATMOSPHERIC
ENVIRONMENT, 46, 299-308, 10.1016/j.atmosenv.2011.09.058, 2012.
- Twomey, S.: Influence of pollution on shortwave albedo of clouds, JOURNAL OF
THE ATMOSPHERIC SCIENCES, 34, 1149-1152,
10.1175/1520-0469(1977)034<1149:tiopot>2.0.co;2, 1977.
- 20 van Donkelaar, A., Martin, R. V., and Park, R. J.: Estimating ground-level PM_{2.5} using
aerosol optical depth determined from satellite remote sensing, JOURNAL OF



- GEOPHYSICAL RESEARCH-ATMOSPHERES, 111, 10.1029/2005jd006996,
2006.
- van Donkelaar, A., Martin, R. V., Brauer, M., Kahn, R., Levy, R., Verduzco, C., and
Villeneuve, P. J.: Global Estimates of Ambient Fine Particulate Matter
5 Concentrations from Satellite-Based Aerosol Optical Depth: Development and
Application, ENVIRONMENTAL HEALTH PERSPECTIVES, 118, 847-855,
10.1289/ehp.0901623, 2010.
- van Donkelaar, A., Martin, R. V., Spurr, R. J. D., Drury, E., Remer, L. A., Levy, R. C.,
and Wang, J.: Optimal estimation for global ground-level fine particulate matter
10 concentrations, JOURNAL OF GEOPHYSICAL RESEARCH-ATMOSPHERES,
118, 5621-5636, 10.1002/jgrd.50479, 2013.
- Wang, J., and Christopher, S. A.: Intercomparison between satellite-derived aerosol
optical thickness and PM_{2.5} mass: Implications for air quality studies,
GEOPHYSICAL RESEARCH LETTERS, 30, 10.1029/2003gl018174, 2003.
- 15 Wang, T., Li, S., Shen, Y., Deng, J., and Xie, M.: Investigations on direct and indirect
effect of nitrate on temperature and precipitation in China using a regional
climate chemistry modeling system, JOURNAL OF GEOPHYSICAL
RESEARCH-ATMOSPHERES, 115, 10.1029/2009jd013264, 2010a.
- Wang, J., Xu, X., Spurr, R., Wang, Y., and Drury, E.: Improved algorithm for MODIS
20 satellite retrievals of aerosol optical thickness over land in dusty atmosphere:
Implications for air quality monitoring in China, REMOTE SENSING OF



- ENVIRONMENT, 114, 2575-2583, 10.1016/j.rse.2010.05.034, 2010b.
- Winker, D. M., Hunt, W. H., and McGill, M. J.: Initial performance assessment of CALIOP, GEOPHYSICAL RESEARCH LETTERS, 34, 10.1029/2007gl030135, 2007.
- 5 Winker, D. M., Vaughan, M. A., Omar, A., Hu, Y., Powell, K. A., Liu, Z., Hunt, W. H., and Young, S. A.: Overview of the CALIPSO Mission and CALIOP Data Processing Algorithms, JOURNAL OF ATMOSPHERIC AND OCEANIC TECHNOLOGY, 26, 2310-2323, 10.1175/2009jtecha1281.1, 2009.
- Xin, J., Gong, C., Liu, Z., Cong, Z., Gao, W., Song, T., Pan, Y., Sun, Y., Ji, D., Wang,
10 L., Tang, G., and Wang, Y.: The observation-based relationships between PM_{2.5} and AOD over China, JOURNAL OF GEOPHYSICAL RESEARCH-ATMOSPHERES, 121, 10701-10716, 10.1002/2015jd024655, 2016.
- Xing, J., Mathur, R., Pleim, J., Hogrefe, C., Gan, C.-M., Wong, D. C., Wei, C., and
15 Wang, J.: Air pollution and climate response to aerosol direct radiative effects: A modeling study of decadal trends across the northern hemisphere, JOURNAL OF GEOPHYSICAL RESEARCH-ATMOSPHERES, 120, 10.1002/2015jd023933, 2015.
- Xu, P., Chen, Y., and Ye, X.: Haze, air pollution, and health in China, LANCET, 382,
20 2067-2067, 2013.
- Yan, Y., Sun, Y. B., Weiss, D., Liang, L. J., and Chen, H. Y.: Polluted dust derived



- from long-range transport as a major end member of urban aerosols and its
implication of non-point pollution in northern China, SCIENCE OF THE
TOTAL ENVIRONMENT, 506, 538-545, 10.1016/j.scitotenv.2014.11.071, 2015.
- Yang, X., Zhao, C., Zhou, L., Wang, Y., and Liu, X.: Distinct impact of different types
5 of aerosols on surface solar radiation in China, JOURNAL OF GEOPHYSICAL
RESEARCH-ATMOSPHERES, 121, 6459-6471, 10.1002/2016jd024938, 2016.
- Zhang, H., Hoff, R. M., and Engel-Cox, J. A.: The Relation between Moderate
Resolution Imaging Spectroradiometer (MODIS) Aerosol Optical Depth and
PM_{2.5} over the United States: A Geographical Comparison by US Environmental
10 Protection Agency Regions, JOURNAL OF THE AIR & WASTE
MANAGEMENT ASSOCIATION, 59, 1358-1369,
10.3155/1047-3289.59.11.1358, 2009a.
- Zhang, M., Song, Y., Cai, X., Lin, W. S., Sui, C. H., Yang, L. M., Wang, X. M., Deng,
R. R., Fani, S. J., Wu, C. S., Wang, A. Y., Fong, S. K., and Lin, H.: A
15 health-based assessment of particulate air pollution in urban areas of Beijing in
2000-2004.
- Zhang, Q., Ma, X., Tie, X., Huang, M., and Zhao, C.: Vertical distributions of aerosols
under different weather conditions: Analysis of in-situ aircraft measurements in
Beijing, China, ATMOSPHERIC ENVIRONMENT, 43, 5526-5535,
20 10.1016/j.atmosenv.2009.05.037, 2009b.
- Zhao, C., Klein, S. A., Xie, S., Liu, X., Boyle, J. S., and Zhang, Y.: Aerosol first



- indirect effects on non-precipitating low-level liquid cloud properties as simulated by CAM5 at ARM sites, GEOPHYSICAL RESEARCH LETTERS, 39, 10.1029/2012gl051213, 2012.
- Zhao, C., and Garrett, T. J.: Effects of Arctic haze on surface cloud radiative forcing, 5 GEOPHYSICAL RESEARCH LETTERS, 42, 557-564, 10.1002/2014gl062015, 2015.
- Zheng, S., Pozzer, A., Cao, C. X., and Lelieveld, J.: Long-term (2001-2012) concentrations of fine particulate matter (PM_{2.5}) and the impact on human health in Beijing, China, ATMOSPHERIC CHEMISTRY AND PHYSICS, 15, 10 5715-5725, 10.5194/acp-15-5715-2015, 2015.
- Zhuang, B. L., Li, S., Wang, T. J., Deng, J. J., Xie, M., Yin, C. Q., and Zhu, J. L.: Direct radiative forcing and climate effects of anthropogenic aerosols with different mixing states over China, ATMOSPHERIC ENVIRONMENT, 79, 349-361, 10.1016/j.atmosenv.2013.07.004, 2013.

15



Table 1. Comparison of AERONET and MODIS AOD by season and over all seasons.

Season	AERONET	MODIS	R ²	Bias	Bias%	RMSE	N
Spring	0.49	0.66	0.81	0.18	36.7	0.23	214
Summer	0.61	0.88	0.87	0.27	44.7	0.29	103
Fall	0.30	0.39	0.69	0.10	32.9	0.15	50
Winter	0.19	0.21	0.34	0.02	10.2	0.08	48
All	0.46	0.63	0.85	0.17	37.8	0.23	415

Note: Bias% is defined as $100 \times (\text{MODIS AOD} - \text{AERONET AOD}) / \text{AERONET AOD}$ (Green et al., 2009). RMSE is the root mean squared prediction error ($\mu\text{g}/\text{m}^3$). Period for comparison is 2011–2015.



Table 2. Comparison of AERONET and CALIPSO AOD by season and over all seasons

Season	AERONET	CALIPSO	R ²	Bias	Bias%	RMSE	<i>N</i>
Spring	0.44	0.42	0.52	-0.02	-5.2	0.33	21
Summer	0.53	0.57	0.47	0.04	6.6	0.32	16
Fall	0.95	0.81	0.85	-0.14	-14.2	0.34	12
Winter	0.42	0.53	0.55	0.11	25.0	0.27	21
All	0.54	0.55	0.65	0.01	1.7	0.31	70



Table 3. Correlations between AOD and PM_{2.5} mass by dominant aerosol specie

Dominant Aerosol Specie	R²	RMSE (µg/m³)	N
Coarse Absorbing	0.56	27.07	480
Mixed Absorbing	0.67	36.44	1383
Fine Absorbing	0.53	48.06	2143
Coarse Non-absorbing	0.10	44.51	56
Mixed Non-absorbing	0.61	44.05	234
Fine Non-absorbing	0.58	40.19	434
All	0.51	46.34	4728



Figure Captions

- Figure 1.** Flow chart of deriving aerosol vertical profile from CALIPSO data.
- Figure 2.** The aerosol classification scheme in four seasons from 2011 to 2015 using AE, SSA and FMF data from AERONET at sites in Beijing. The scatter plots of different colors is the distribution of aerosol types with different physic-optics characteristics in four seasons.
- Figure 3.** Scatter plots of AERONET AOD vs. MODIS AOD (a), and AERONET AOD vs. CALIPSO AOD (b) for the period of 2011 to 2015 in Beijing.
- Figure 4.** Comparison of monthly averaged RH and PBLH (a), AOD and $PM_{2.5}$ (b), AOD_{dry} and $PM_{2.5_column}$ (c) at 14:00 LT for the period of 2011 to 2015 in Beijing.
- Figure 5.** Diurnal variations of multi-year (2011-2015) averaged RH and PBLH over four seasons in Beijing.
- Figure 6.** Comparison of multi-year (2011-2015) averaged RH and PBLH (a1~d1), AOD and $PM_{2.5}$ (a2~d2), AOD_{dry} and $PM_{2.5_column}$ (a3~d3) by time of day in different seasons. The columns represent four seasons and the rows represent three different variables.
- Figure 7.** The frequency distribution of aerosol types over four seasons for the period of 2011 to 2015 in Beijing.
- Figure 8.** The variation of η with the aerosol type in four seasons for the period of 2011 to 2015.
- Figure 9.** Scatter plots between AERONET AOD and $PM_{2.5}$ concentrations in four different seasons for six different types of aerosols. The first to 6th columns represent the aerosol types of coarse absorbing, mixed absorbing, fine absorbing, coarse non-absorbing, mixed non-absorbing and fine non-absorbing, respectively. The colors also represent different aerosol types. The rows represent four seasons.
- Figure 10.** Wind rose of Beijing in four seasons for the period of 2011 to 2015
- Figure 11.** The relative distribution of AOD (upper panel) and $PM_{2.5}$ (lower panel) within different value ranges at Beijing for different surface wind speed ranges from 2011 to 2015. v and N represent the wind speed and samples respectively. The colors represent the value ranges of AOD (upper panel) and $PM_{2.5}$ (lower panel).
- Figure 12.** Variation of averaged AOD, $PM_{2.5}$ (left panel) and η (right panel) with the surface wind speed.
- Figure 13.** Aerosol vertical distribution profile (a), and aerosol cumulative distribution from high to low with altitude (b) in four seasons. The colors represent different seasons.



Figure 14. The normalized vertical distribution of AOD in four seasons. h values shown in each panels are the heights with the highest AOD contribution (percentage). The colors represent different seasons.

Figure 15. Scatter plots of stratified AOD vs. PM_{2.5} concentrations. The red solid line is the linear fitting regression lines. It shows the relationship between (a) AOD below 500m, (b) AOD below 1000m, (c) AOD below PBL and (d) AOD of the whole atmosphere and PM_{2.5} concentrations.

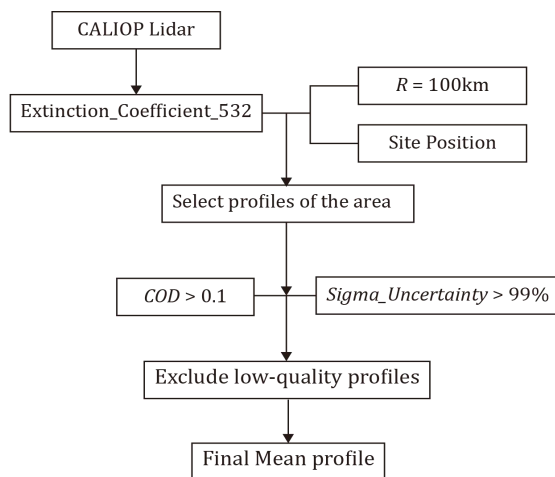


Figure 1. Flow chart of deriving aerosol vertical profile from CALIPSO data.

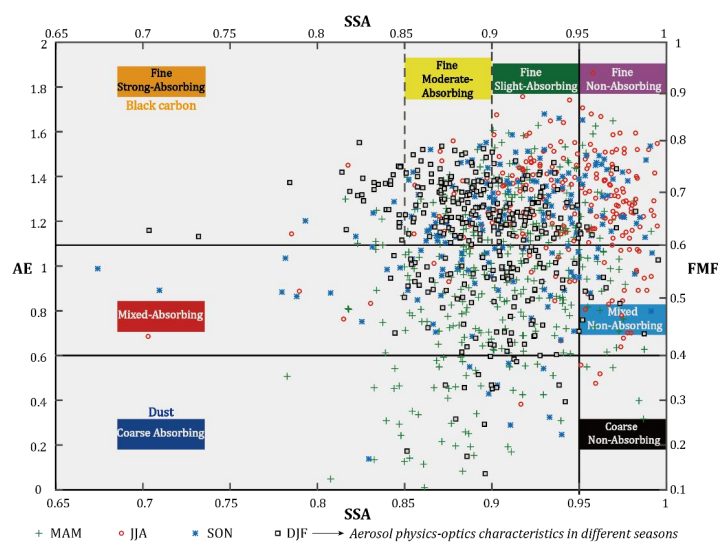


Figure 2. The aerosol classification scheme in four seasons from 2011 to 2015 using AE, SSA and FMF data from AERONET at sites in Beijing. The scatter plots of different colors is the distribution of aerosol types with different physico-optics characteristics in four seasons.

5

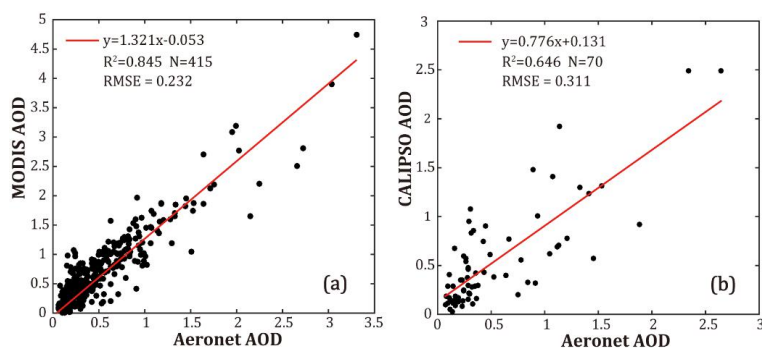


Figure 3. Scatter plots of AERONET AOD vs. MODIS AOD (a), and AERONET AOD vs. CALIPSO AOD (b) for the period of 2011 to 2015 in Beijing.

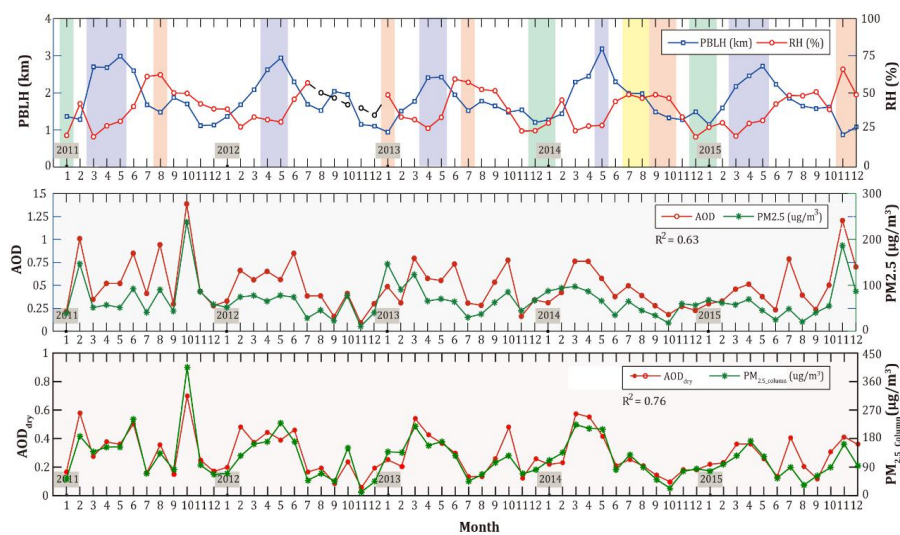


Figure 4. Comparison of monthly averaged RH and PBLH (a), AOD and $PM_{2.5}$ (b), AOD_{dry} and $PM_{2.5_column}$ (c) at 14:00 LT for the period of 2011 to 2015 in Beijing.

5

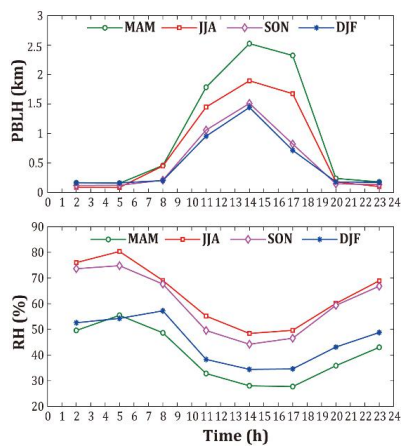


Figure 5. Diurnal variations of multi-year (2011-2015) averaged RH and PBLH over four seasons in Beijing.

5

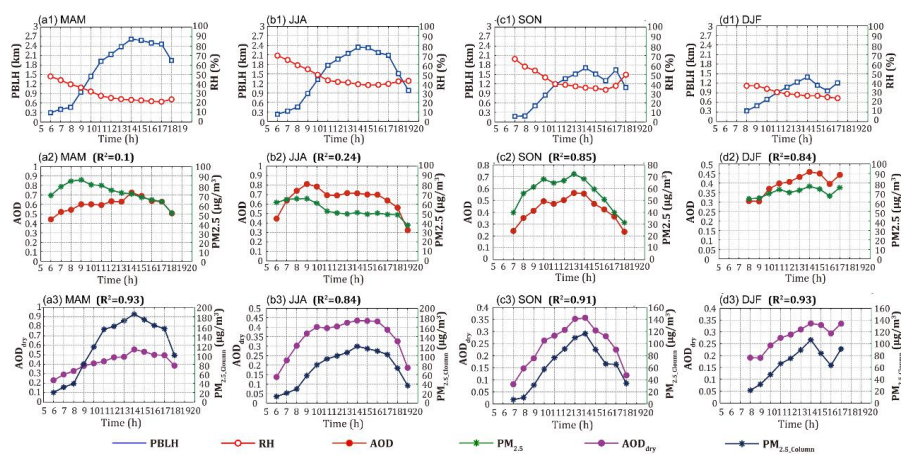


Figure 6. Comparison of multi-year (2011-2015) averaged RH and PBLH (a1~d1), AOD and $PM_{2.5}$ (a2~d2), AOD_{dry} and $PM_{2.5_column}$ (a3~d3) by time of day in different seasons. The columns represent four seasons and the rows represent three different variables.

5

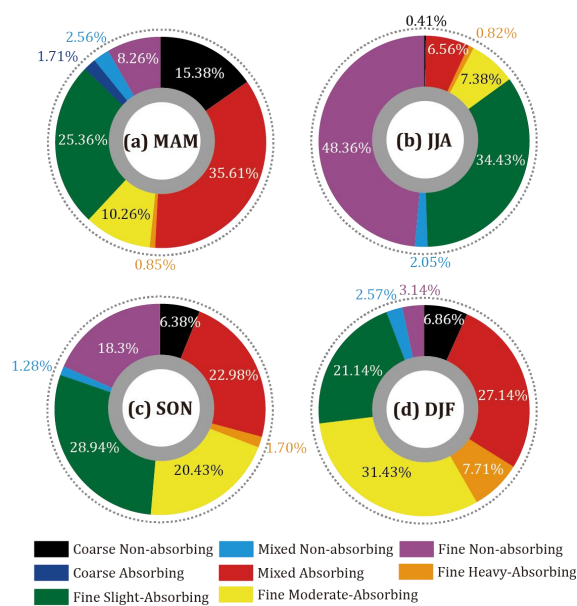


Figure 7. The frequency distribution of aerosol types over four seasons for the period of 2011 to 2015 in Beijing.

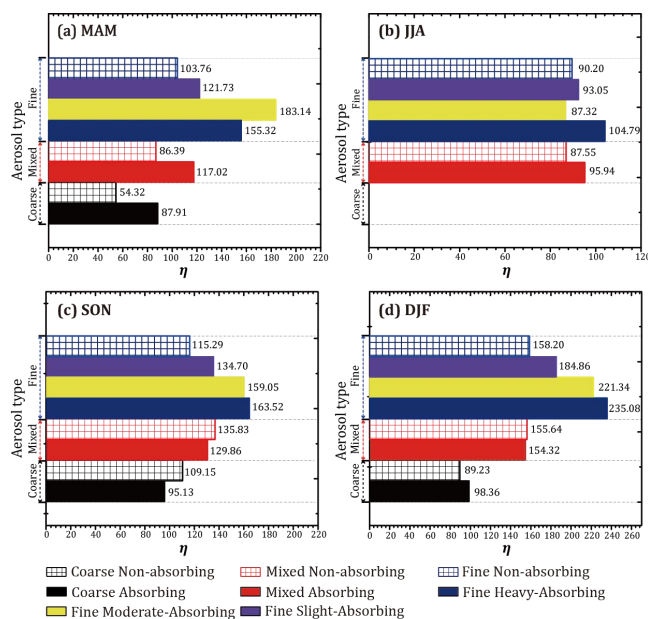


Figure 8. The variation of η with the aerosol type in four seasons for the period of 2011 to 2015.

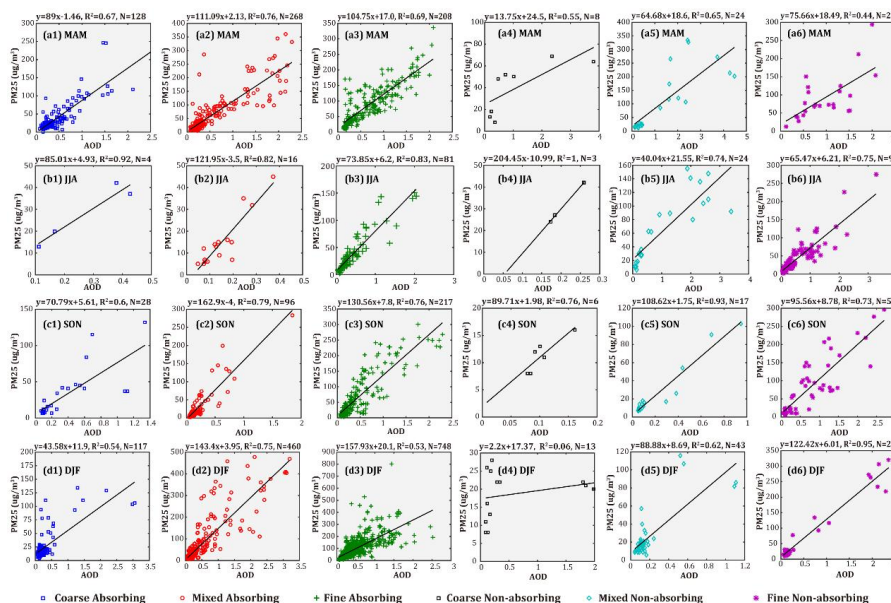


Figure 9. Scatter plots between AERONET AOD and PM_{2.5} concentrations in four different seasons for six different types of aerosols. The first to 6th columns represent the aerosol types of coarse absorbing, mixed absorbing, fine absorbing, coarse non-absorbing, mixed non-absorbing and fine non-absorbing, respectively. The colors also represent different aerosol types. The rows represent four seasons

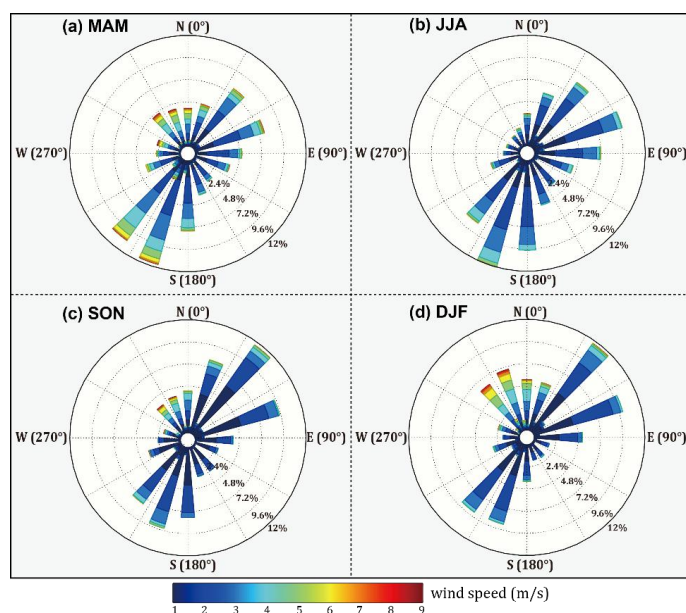


Figure 10. Wind rose of Beijing in four seasons for the period of 2011 to 2015

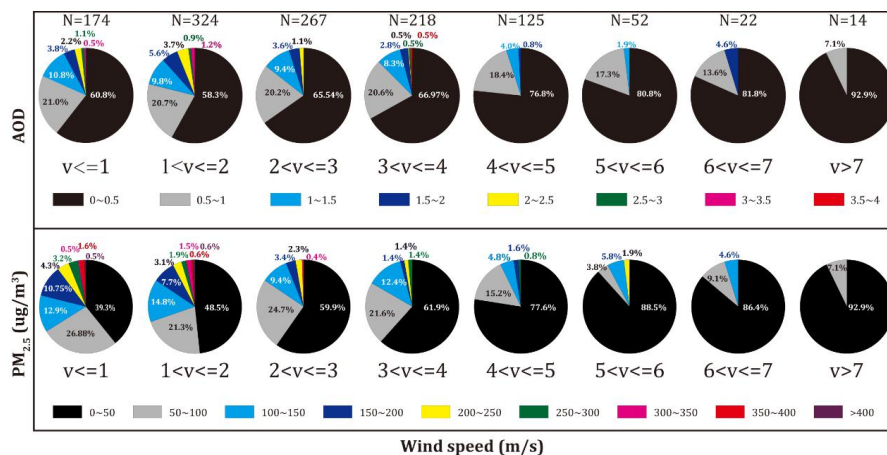


Figure 11. The relative distribution of AOD (upper panel) and PM_{2.5} (lower panel) within different value ranges at Beijing for different surface wind speed ranges from 2011 to 2015. v and N represent the wind speed and samples respectively. The colors represent the value ranges of AOD (upper panel) and PM_{2.5} (lower panel).

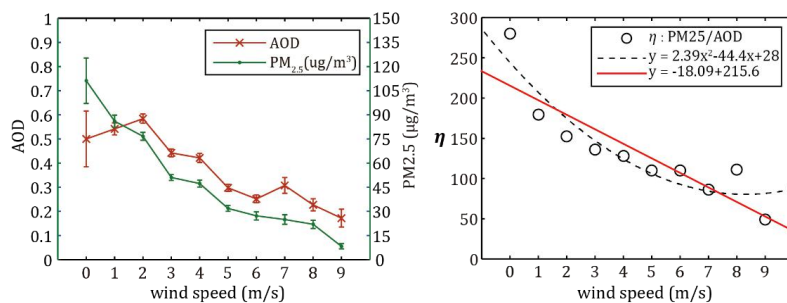


Figure 12. Variation of averaged AOD, PM_{2.5} (left panel) and η (right panel) with the surface wind speed.

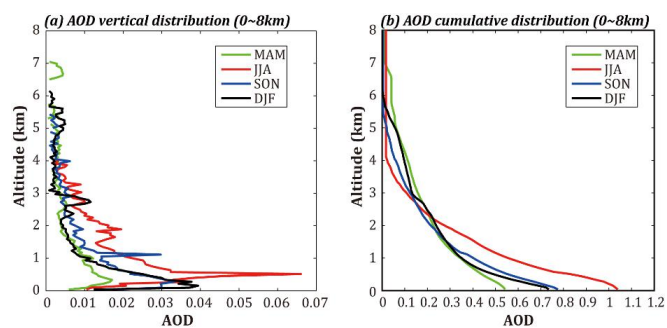


Figure 13. Aerosol vertical distribution profile (a), and aerosol cumulative distribution from high to low with altitude (b) in four seasons. The colors represent different seasons.

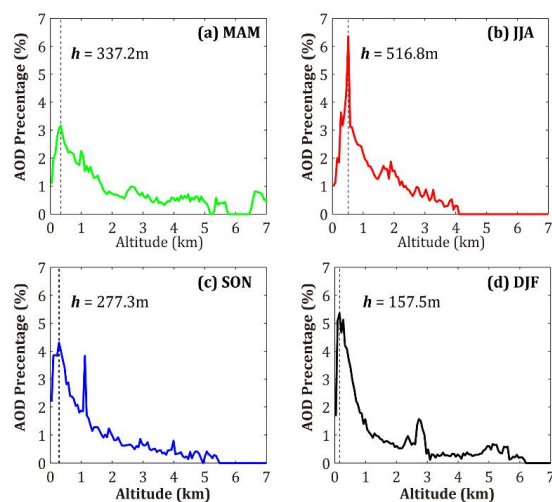


Figure 14. The normalized vertical distribution of AOD in four seasons. h values shown in each panels are the heights with the highest AOD contribution (percentage). The colors represent different seasons.

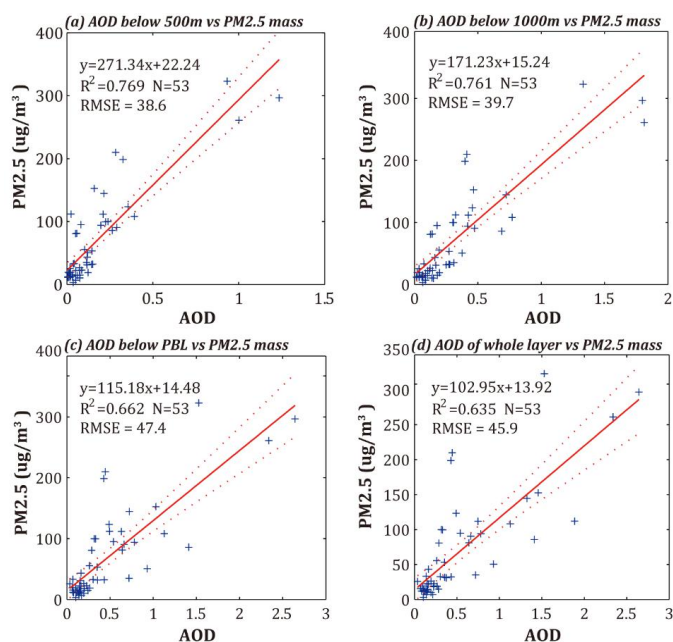


Figure 15. Scatter plots of stratified AOD vs. PM2.5 concentrations. The red solid line is the linear fitting regression lines. It shows the relationship between (a) AOD below 500m, (b) AOD below 1000m, (c) AOD below PBL and (d) AOD of the whole atmosphere and PM2.5 concentrations.